Journal of Materials and Environmental Sciences
ISSN : 2028-2508



JMES, 2017 Volume 8, Issue 4, Page 1291-1300

http://www.jmaterenvironsci.com/

# Theoretical investigation of new pyrimidines π-conjugated based materials for photovoltaic applications

**Z. El Aslaoui[1], Y. Karzazi[1, 2 *]**

*1Laboratory of Applied Analytical Chemistry Materials and Environment, Faculty of Sciences, University Mohammed Premier, P. O. Box 4808, 60046 Oujda, Morocco.*
*2LSIA, National School of Applied Sciences, ENSA Al Hoceima, University Mohammed Premier, P. O. Box 3, 32003 SidiBouafif, Morocco.*

*Received 29Aug 2016,*
*Revised 01Oct 2016,*
Accepted 04 Oct 2016

*Keywords*
- ✓ HOMO,
- ✓ LUMO,
- ✓ Solar cells,
- ✓ Open circuit voltage,
- ✓ Oscillator strength,
- ✓ UV-Vis,
- ✓ DFT,
- ✓ TD/DFT,

karzazi@hotmail.com

## Abstract

The pyrimidine-based compounds and derivatives are among the organic luminescent compounds that become very good candidates for new technologies such as organic light emitting diodes and solar cells. In this work, full geometry optimization with no constraints of pyrimidine derivatives were performed using the Density Functional Theory (DFT) based on Beck's three-parameter exchange functional and Lee–Yang–Parr nonlocal correlation functional (B3LYP) and the 6-31G(d, p) orbital basis sets for all atoms as implemented in Gaussian 09 program. The Molecular properties estimated include the highest occupied molecular orbital (HOMO), lowest unoccupied molecular orbital (LUMO), and other molecular properties derived from HOMO and LUMO and their respective energies. Besides, Time-Dependent Density Functional Theory (TD/DFT) calculations were used to enumerate the absorption properties like the maximum absorption wavelengths, the excitation energy and oscillator strengths corresponding to the pyrimidine derivatives. We have also calculated the open circuit voltage and the difference between both the LUMO energy levels of the donor and the acceptor. Hence, the aim of this study is to evidence the relationship between the chemical structure of the pyrimidine based materials and their optoelectronic properties behaviors and finally to conceive the compounds with effective character for solar cells. Our results lead to the likelihood to suggest pyrimidine based materials as bulk-heterojunction solar cell for organic solar cells application because the electron injection process from the studied molecules to the conduction band of the acceptor and the subsequent regeneration are possible.

## 1. Introduction

The conversion of solar energy directly into electricity is one of the most attractive renewable energy sources that can help replace fossil fuels and control global warming [1, 2]. New solar cells based on organic compounds are a subject of an increasing interest in recent years due to their advantages of low cost fabrication by using solution processing techniques at low temperature and avoiding costly vacuum processes, light weight, processability of organic materials and potential to make flexible photovoltaic devices in comparison with the traditional silicon-based solar cells [3-5]. However, the power conversion efficiency (PCE) and device performances are limited by the low exciton dissociation as well as low charge collection [6, 7]. To overcome these limitations, we can put bulk heterojunction (BHJ) (a blend of both donor and acceptor materials dispersed through the photoactive region) which is based on the conjugated molecules. Recently these conjugated molecules have been the subject of much research due to the growing interest in advanced photonic applications, low-cost, flexible and lightweight materials such as electroluminescent devices [8, 9], and photovoltaics [10-12]. To date, the most promising organic solar cells are based on composite of an electron-donor conjugated polymer and electron-acceptor fullerene with power conversion efficiency (PCE) nearly 10.6% [13, 14]. Nevertheless, despite the progress in terms of PCE, the short life time of organic solar cells limits considerably their commercial production in large scale. Researches were recently devoted to understand degradation mechanisms in organic solar cells in order to improve the stability and then the life time of OPV devices [15, 16]. In this work, we present theoretical study of the structural and optoelectronic properties of new

systems based on pyrimidine derivatives by quantum chemistry using DFT (Density Functional Theory) and B3LYP hybrid functional density to obtain full geometries optimization. The absorption spectra were simulated by TD/DFT (Time Dependent Density Functional Theory). With the goal to find potential sensitizers for a good use in organic solar cells, pyrimidine based compounds were studied. Different electron side groups (polyoxadiazol and polythiophen) were introduced to investigate their effects on the electronic structure. Hence, electronic and optical properties have been reported in order to predict the BHJ solar cell device efficiency for the studied compounds [17, 18]. Hence, we will scan the rapport between the molecular, the electronic structure and the efficiency of the solar cell in order to give further insights on the possibility of electron transfer between the donor and the acceptor entities in the pyrimidines π-conjugated based materials.

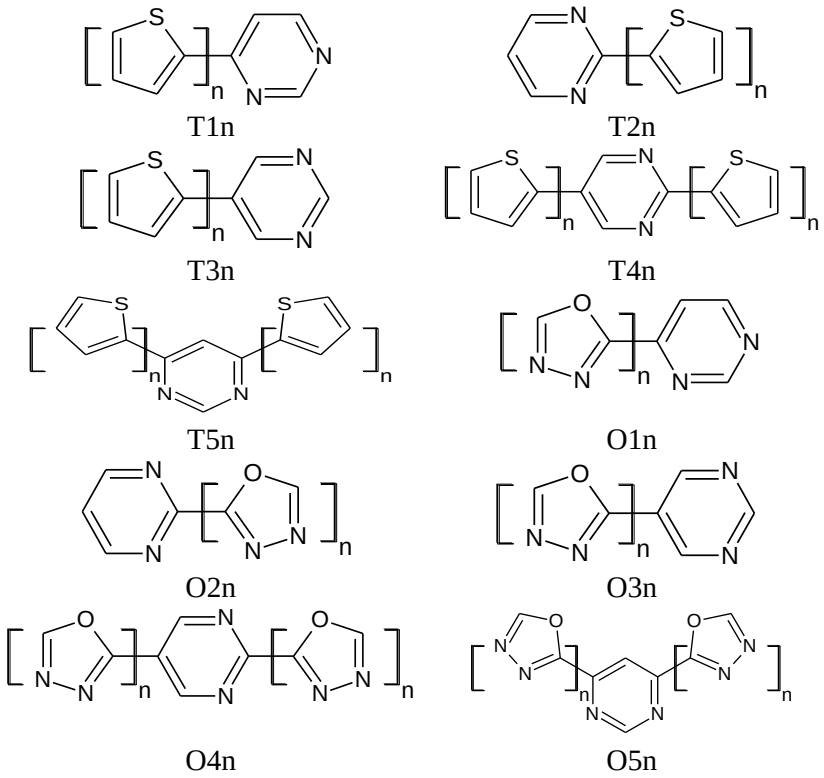


**Figure 1:**Structures of the studied molecules (where n=1, 2, 3).

## 2. Materials and methods

Full geometry optimizations of pyrimidine π-conjugated based derivatives (figure 1) at ground states were performed under no constraints in the structure with the Density Functional Theory (DFT) based on Beck's three-parameter exchange functional and Lee–Yang–Parr nonlocal correlation functional (B3LYP) [19-21] and the 6-31G (d, p) orbital basis sets for all atoms as implemented in Gaussian 09 program [22] supported by Gauss View 5.0 interface [23] for a visual presentation of the graphics. The highest occupied molecular orbital (HOMO) and the lowest unoccupied molecular orbital (LUMO) levels of the compounds under study were calculated and compared to LUMO of PCEM and PCBM, the gap energy is evaluated as the difference between the HOMO and LUMO energies ($E_{gap} = E_{LUMO} - E_{HOMO}$). Calculated values of HOMO, LUMO, $E_{gap}$ and $V_{oc}$ (open circuit voltage), corresponding to the tested compounds, are fundamental in the study of organic solar cells. Vertical electronic excitation spectra, including maximal wavelengths (λmax), oscillators strengths (O.S) and excitation energy (Ex) were systematically investigated using TD/DFT for instance B3LYP/6-31G(d) method, on the basis of the optimized ground state structures. Noteworthy, all calculations were carried out in the gas phase.

## 3. Results and discussion

*3.1. Geometry optimization*

The optimized structures of all studied compounds are illustrated in figure 2. The results of the optimized structures for the compounds under study show that they have similar quasi planar conformations. We found also that the modification of the kind and position of substitution on the pyrimidine ring does not change the geometric parameters and especially the planar conformation for all the molecules under study.

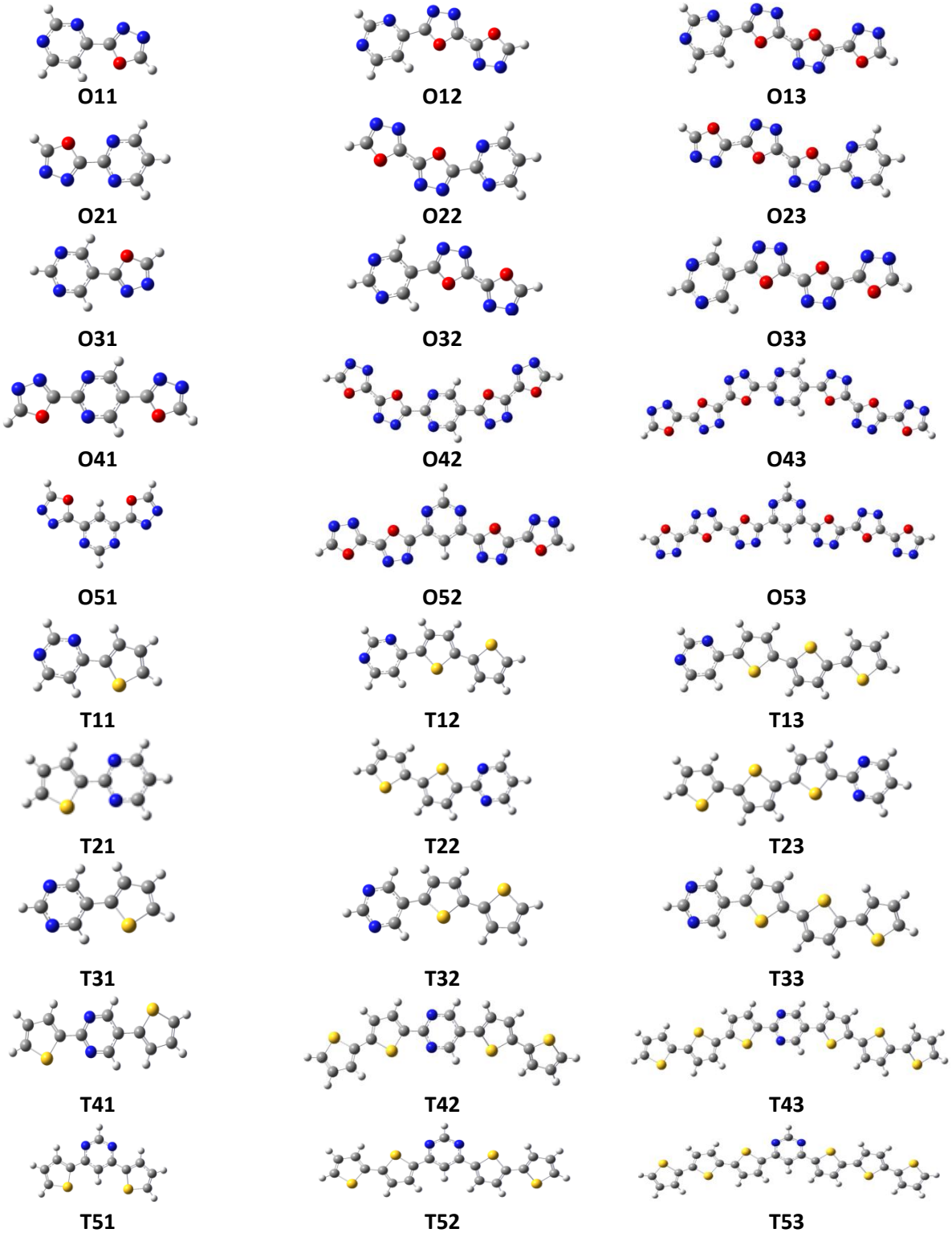


**Figure 2:**Optimized geometries of the studied molecules as calculated at the B3LYP/6-31G (d, p) level.

*3.2. Electronic properties*

It's important to examine characters of the frontier orbitals because the relative ordering of the occupied and virtual orbitals provides a reasonable qualitative indication of the excitation properties and of the ability of electron or hole transport [24, 25]. The HOMOs and LUMOs of all studied molecules gathered in Figure 3, show that the HOMOs possess a π-bonding character within subunit and a π-antibonding character between the consecutive subunits while the LUMOs generally indicate a π-antibonding character within subunit and a π-bonding character between the subunits and therefore, the compounds investigated in this paper will have aromatic character. We noted also that HOMO and LUMO cover, generally, the entire backbone of the molecules under study.

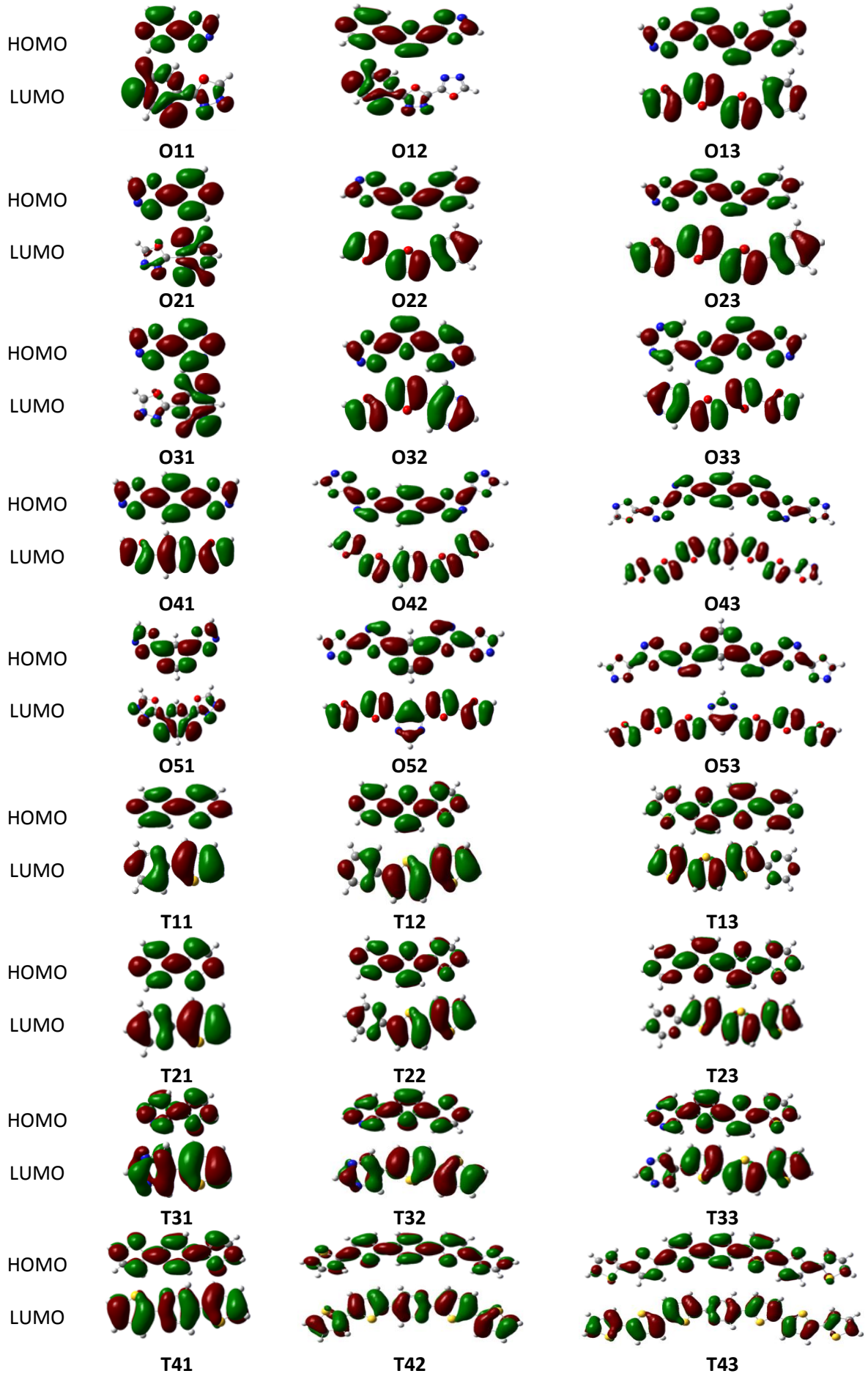
HOMO
LUMO
O11
O12
O13
HOMO
LUMO
O21
O22
O23
HOMO
LUMO
O31
O32
O33
HOMO
LUMO
O41
O42
O43
HOMO
LUMO
O51
O52
O53
HOMO
LUMO
T11
T12
T13
HOMO
LUMO
T21
T22
T23
HOMO
LUMO
T31
T32
T33
HOMO
LUMO
T41
T42
T43

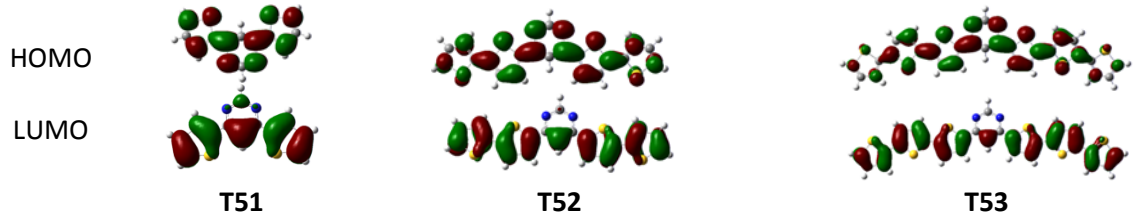


**Figure 3:** The contour plots of HOMO and LUMO orbitals of the studied compounds.

Table 1 lists the calculated frontier orbital energies and energy gap ($E_{gap}$) between highest occupied molecular orbital (HOMO) and lowest unoccupied molecular orbital (LUMO) of the studied molecules.

**Table 1:** Calculated frontier orbital energies, energy gap and open circuit voltage ($E_{HOMO}$, $E_{LUMO}$, $E_{gap}$ and $V_{oc}$) at the B3LYP/6-31G (d, p) level for the studied molecules.

| Molecules | $E_{HOMO}$ (eV) | $E_{LUMO}$ (eV) | $E_{gap}$ (eV) | $V_{OC}$ (eV) PCBM | α (eV) PCBM | $V_{OC}$ (eV) PCEM | α (eV) PCEM |
|---|---|---|---|---|---|---|---|
| **O11** | -7.30 | -2.32 | 4.99 | 3.30 | 1.39 | 2.9 | 1.78 |
| **O12** | -7.44 | -2.78 | 4.66 | 3.44 | 0.92 | 3.04 | 1.32 |
| **O13** | -7.49 | -3.07 | 4.42 | 3.49 | 0.63 | 3.09 | 1.03 |
| **O21** | -7.26 | -2.03 | 5.23 | 3.26 | 1.68 | 2.86 | 2.07 |
| **O22** | -7.27 | -2.51 | 4.76 | 3.27 | 1.19 | 2.87 | 1.59 |
| **O23** | -7.27 | -2.84 | 4.44 | 3.27 | 0.86 | 2.87 | 1.26 |
| **O31** | -7.31 | -2.12 | 5.19 | 3.31 | 1.58 | 2.91 | 1.98 |
| **O32** | -7.38 | -2.66 | 4.72 | 3.38 | 1.04 | 2.98 | 1.44 |
| **O33** | -7.39 | -3.01 | 4.37 | 3.39 | 0.69 | 2.99 | 1.09 |
| **O41** | -7.31 | -2.78 | 4.53 | 3.31 | 0.92 | 2.91 | 1.32 |
| **O42** | -7.30 | -3.26 | 4.04 | 3.30 | 0.44 | 2.90 | 0.84 |
| **O43** | -7.35 | -3.48 | 3.87 | 3.35 | 0.22 | 2.95 | 0.62 |
| **O51** | -7.60 | -2.82 | 4.78 | 3.60 | 0.88 | 3.20 | 1.28 |
| **O 52** | -7.56 | -3.21 | 4.36 | 3.56 | 0.49 | 3.16 | 0.89 |
| **O53** | -7.54 | -3.42 | 4.12 | 3.54 | 0.28 | 3.14 | 0.68 |
| **T11** | -6.36 | -1.79 | 4.56 | 2.36 | 1.91 | 1.96 | 2.31 |
| **T12** | -5.69 | -2.08 | 3.61 | 1.69 | 1.62 | 1.29 | 2.02 |
| **T13** | -5.36 | -2.24 | 3.13 | 1.36 | 1.46 | 0.96 | 1.86 |
| **T21** | -6.08 | -1.52 | 4.56 | 2.08 | 2.18 | 1.68 | 2.58 |
| **T22** | -5.45 | -1.84 | 3.61 | 1.45 | 1.86 | 1.05 | 2.26 |
| **T23** | -5.17 | -2.03 | 3.14 | 1.17 | 1.67 | 0.77 | 2.07 |
| **T31** | -6.30 | -1.56 | 4.74 | 2.30 | 2.14 | 1.90 | 2.54 |
| **T32** | -5.67 | -1.91 | 3.76 | 1.67 | 1.79 | 1.27 | 2.19 |
| **T33** | -5.35 | -2.11 | 3.23 | 1.35 | 1.59 | 0.95 | 1.99 |
| **T41** | -5.76 | -1.83 | 3.93 | 1.76 | 1.87 | 1.36 | 2.27 |
| **T42** | -5.25 | -2.16 | 3.09 | 1.25 | 1.54 | 0.85 | 1.94 |
| **T43** | -5.04 | -2.30 | 2.74 | 1.04 | 1.40 | 0.64 | 1.8 |
| **T51** | -6.22 | -1.90 | 4.32 | 2.22 | 1.80 | 1.82 | 2.2 |
| **T52** | -5.52 | -2.19 | 3.33 | 1.52 | 1.51 | 1.12 | 1.91 |
| **T53** | -5.22 | -2.32 | 2.90 | 1.22 | 1.38 | 0.82 | 1.78 |

The energy gap of the studied molecules based on pyrimidine substituted by oxadiazol drops from 5.23 eV (for O21) to 3.87 eV (for O43). The results assembled in Table 1 show a band gap decline when the length of conjugation is augmented and the subsequent tendencies are perceived: 4.99 eV, 4.66 eV and 4.42 eV for O11, O12 and O13 respectively, 5.23 eV, 4.76 eV and 4.44 eV for O21, O22 and O23 respectively, 5.19 eV, 4.72 eV and 4.37 eV for O31, O32 and O33 respectively, 4.53 eV, 4.04 eV and 3.87 eV for O41, O42 and O43

respectively, and lastly 4.78 eV, 4.36 eV and 4.12 eV for O51, O52 and O53 respectively. In addition, the energy gap of the studied molecules based on pyrimidine substituted by polythiophen decreases from 4.74 eV (for T31) to 2.74 eV (for T43). The results gathered in Table 1 show a bandgap decrease when the length of conjugation is increased and the following trends are observed: 4.56 eV, 3.61 eV and 3.13 eV for T11, T12 and T13 respectively, 4.56 eV, 3.61 eV and 3.14 eV for T21, T22 and T23 respectively, 4.74 eV, 3.76 eV and 3.23 eV for T31, T32 and T33 respectively, 3.93 eV, 3.09 eV and 2.74 eV for T41, T42 and T43 compounds respectively, and finally 4.32 eV, 3.33 eV and 2.90 eV for T51, T52 and T53 respectively. The different structures play key roles on electronic properties and the effect of slight structural variations, especially the effect of the motifs branched to the pyrimidine molecule on the HOMO and LUMO energies is clearly seen.

Figures 4 and 5 display the evolution of the calculated HOMO and LUMO energies as a function of reciprocal chain length for the series of pyrimidine-(oxadiazol)$_n$ and pyrimidine-(thiophen)$_n$ under study. With the results presented in Figures 6 and 7 we can emphasize that the HOMO energies are destabilized with the increase of the conjugation length, whereas the LUMO energies are stabilized. These results indicate that the chain length of polymers has a big effect on electronic transition. We highlight also that there is a linear correlation between the energy gap and the inverse chain length as exhibited in Figures 6 and 7. In fact, there is a good linear relation (about $r2 = 0.99$) between the energy gap and the inverse chain length. In theory, the bandgap of the polymer is the orbital energy difference between the HOMO and the LUMO when the repeated unit number is infinite. For our molecules under study, the values of bandgap, calculated using Figures 6 and 7, will be between 3.54 eV and 4.14 eV for the series of pyrimidine-(oxadiazol)n and between 2.16 eV and 2.49 eV for the series of pyrimidine-(thiophen)$_n$. Therefore, for the pyrimidine-(thiophen)$_n$ (respectively, pyrimidine-(oxadiazol)$_n$) derivatives, the molecule T43 (respectively, O43) has the smallest bandgap suggesting this compound to have the most outstanding photophysical properties.

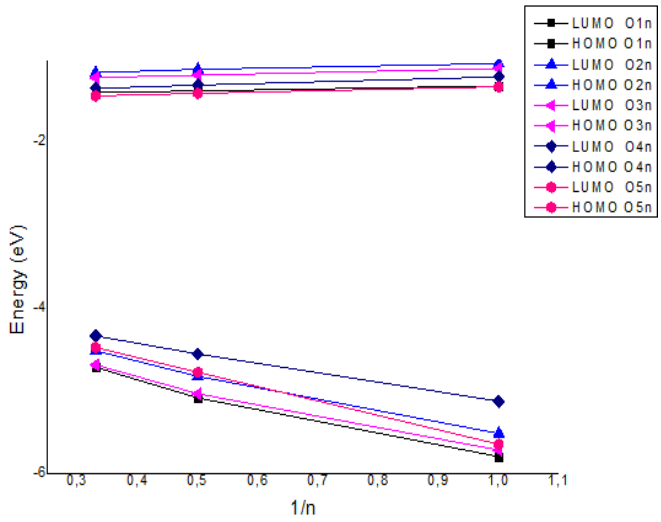


**Figure 4**: HOMO and LUMO energies calculated at B3LYP/6-31G (d, p) level as a function of reciprocal chain length n of pyrimidine-(oxadiazol)$_n$.

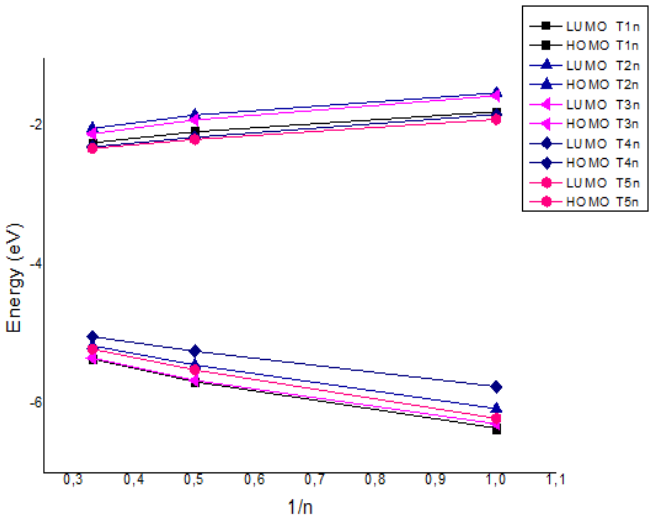


**Figure 5:** HOMO and LUMO energies calculated at B3LYP/6-31G (d, p) level as a function of reciprocal chain length n of pyrimidine-(thiophen)$_n$.

3.2. *Photovoltaic properties*

Figures 6 and 7 show detailed data of absolute energy of the frontier molecular orbitals for O11, O12, O13, O21, O22, O23, O31, O32, O33, O41, O42, O43, O51, O52, O53, T11, T12, T13, T21, T22, T23, T31, T32, T33, T41, T42, T43, T51, T52 and T53, as well as ITO, PCEM, PCBM and Al which are included in order to evaluate the possibilities of electron transfer from the studied molecules to the conductive band of PCEM or PCBM and also for comparison purposes. It is deduced that substitution pushes up/down the HOMO/LUMO energies in agreement with their electron donor/acceptor character. Therefore, we conclude that the LUMO (respectively, HOMO) energy levels of the pyrimidine-polyoxadiazol are destabilized (respectively, stabilized). Contrariwise, the LUMO (respectively, HOMO) energy levels of the pyrimidine-polythiophen based materials are stabilized (respectively, destabilized). Besides, the HOMO levels of the studied compounds were lower than that of PCEM or PCBM while the LUMO levels were higher than that of PCEM or PCBM.

The LUMO energy levels of the studied pyrimidine-polythiophen based molecules are much higher than that of ITO conduction band edge (-4.7 eV). Thus, molecules in excited states of T11, T12, T13, T21, T22, T23, T31, T32, T33, T41, T42, T43, T51, T52 and T53 have a strong ability to inject electrons into ITO electrodes. The

increase of the HOMO levels may suggest a negative effect on organic solar cell performance due to the broader gap between the HOMO level of the organic molecules and the HOMO level of PCEM or PCBM [26, 27].

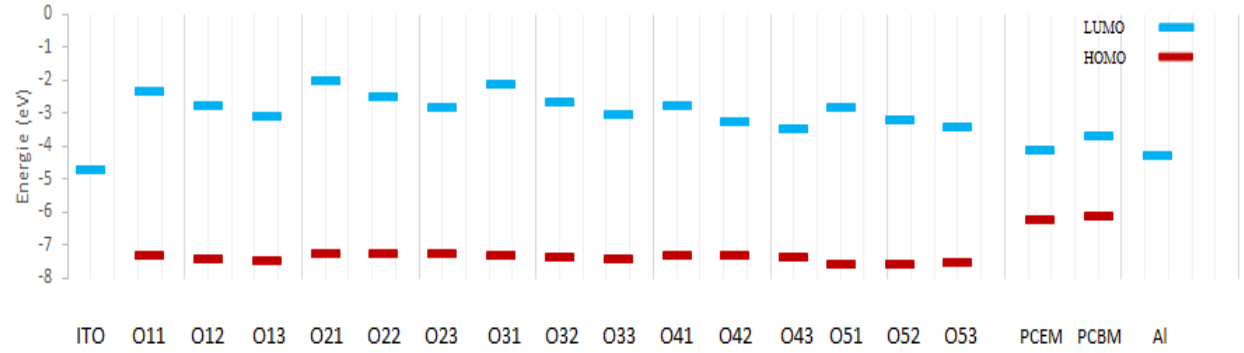


**Figure 6:** HOMO and LUMO energy levels of PCEM, PCBM and pyrimidine-(oxadiazol)n, as calculated at the DFT/B3LYP/6-31G (d, p) level.

Both HOMO and LUMO levels of the studied molecules agree well with the requirement for an efficient photosentizer. It should be noted that the HOMO and LUMO levels of the pyrimidine-polythiophen based molecules under study are higher than that of PCEM or PCBM [28] (which varies in literature from -3.8 to -4.3 eV).

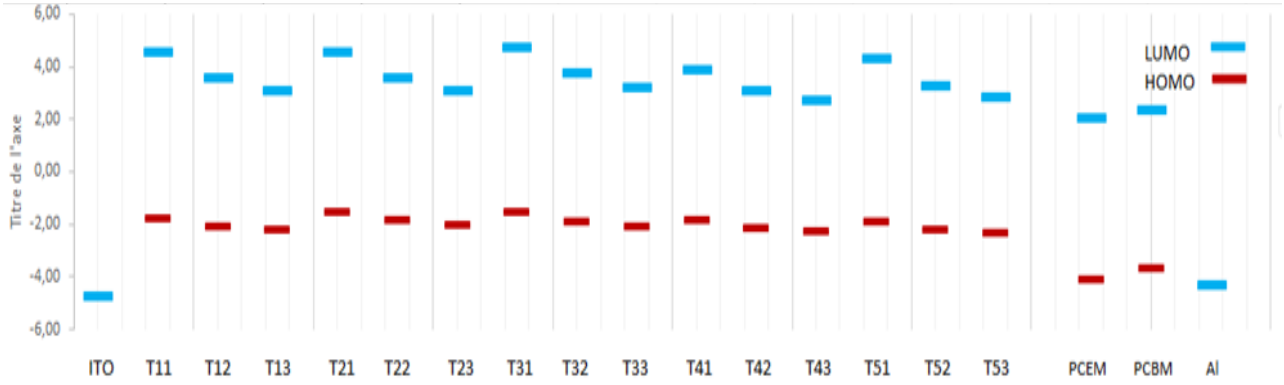


**Figure 7:** HOMO and LUMO energy levels of PCEM, PCBM and pyrimidine-(thiophen)n, as calculated at the DFT/B3LYP/6-31G (d, p) level.

The power conversion efficiency (PCE) was calculated according to the following equation (1):

$$PCE = \frac{1}{P_{in}\ (FF\ .V_{OC}\ .J_{SC}\ )} \qquad (1)$$

Where Pin is the incident power density, Jsc is the short-circuit current, Voc is the open-circuit voltage, and FF denotes the fill factor. To evaluate the possibilities of electron transfer from the excited studied molecules to the conductive band of PCBM, the HOMO and LUMO levels are compared. Knowing that in organic solar cells, the open circuit voltage is found to be linearly dependent on the HOMO level of the donor and the LUMO level of the acceptor. The maximum open circuit voltage (Voc) of the BHJ solar cell is related to the difference between the highest occupied molecular orbital (HOMO) of the donor (our studied molecules) and the LUMO of the electron acceptor (PCBM or PCEM), taking into account the energy lost during the photo-charge generation [29]. The theoretical values of open-circuit voltage Voc have been calculated from the following expression:

$$V_{OC} = |E_{HOMO}\ (\text{Donor})| - |E_{LUMO}\ (\text{Acceptor})| - 0{,}3 \qquad (2)$$

The obtained values of $V_{oc}$ of the studied molecules calculated according to the equation (2) range from 3.26 eV to 3.6 eV for the pyrimidine (oxadiazol)n based derivatives and from 1.04 eV to 2.36 eV for the pyrimidine-(thiophen)n based derivatives when considering PCBM as the acceptor and from 2.86 eV to 3.2 eV for the pyrimidine-(oxadiazol)n based derivatives and from 0.64 eV to 1,96 eV for the pyrimidine-(thiophen)n based derivatives when considering PCEM as the acceptor (see Table 1). Provided that energy gap of 0.2 eV is

necessary for efficient electron injection, these values are sufficiently large for effective electron injection. Therefore, the studied molecules can be used as sensitizers because the electron injection process from the excited molecule to the conduction band of PCEM or PCBM and the subsequent regeneration are feasible in organic sensitized solar cell. Besides, to efficiently inject the electron into the conduction band of PCBM or PCEM; the value of LUMO Donor must be greater than that of PCEM or PCBM and accordingly α must be positive [30-33]. This condition is fulfilled for the studied molecules as it can be verified in Table 1.

*3.3. Absorption properties*

The absorption properties of a new material matches with the solar spectrum is an important factor for the application as a photovoltaic material, and a good photovoltaic material should have broad and strong visible absorption characteristics [32]. The TD/DFT method has been used on the basis of the optimized geometry to obtain the energy of the singlet–singlet electronic transitions and absorption properties (λmax) of O11, O12, O13, O21, O22, O23, O31, O32, O33, O41, O42, O43, O51, O52, O53, T11, T12, T13, T21, T22, T23, T31, T32, T33, T41, T42, T43, T51, T52 and T53. As illustrated in figures 8 and 9, we can find the values of calculated wavelength λmax and oscillator strengths O.S of the pyrimidine-(oxadiazol)n and the pyrimidine-(thiophen)n based derivatives.

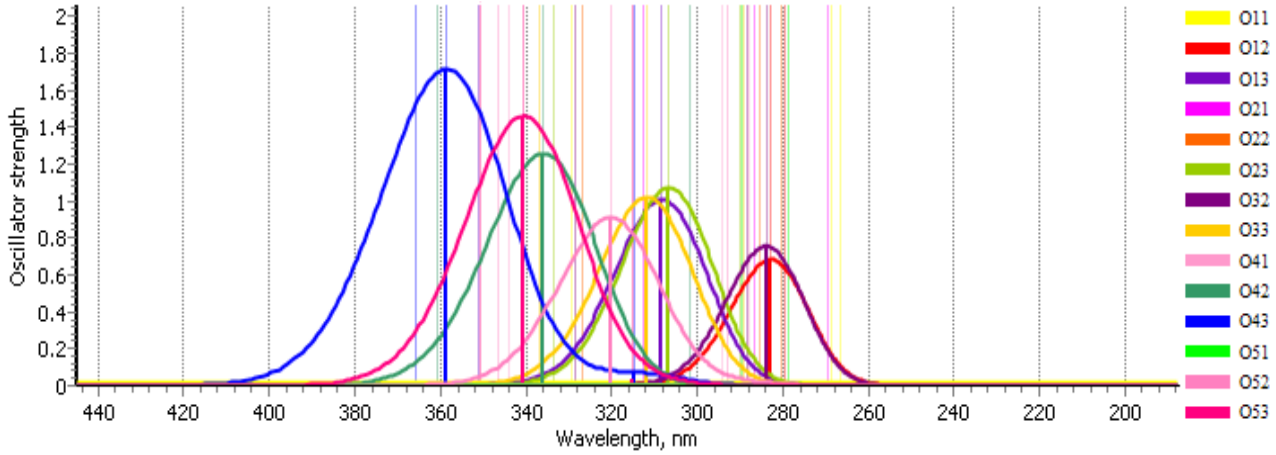


**Figure 8:**Simulated UV-visible optical absorption spectra of each compound of the pyrimidine-(oxadiazol)n based derivatives at the TD/DFT B3LYP/6-31G(d,p) level.

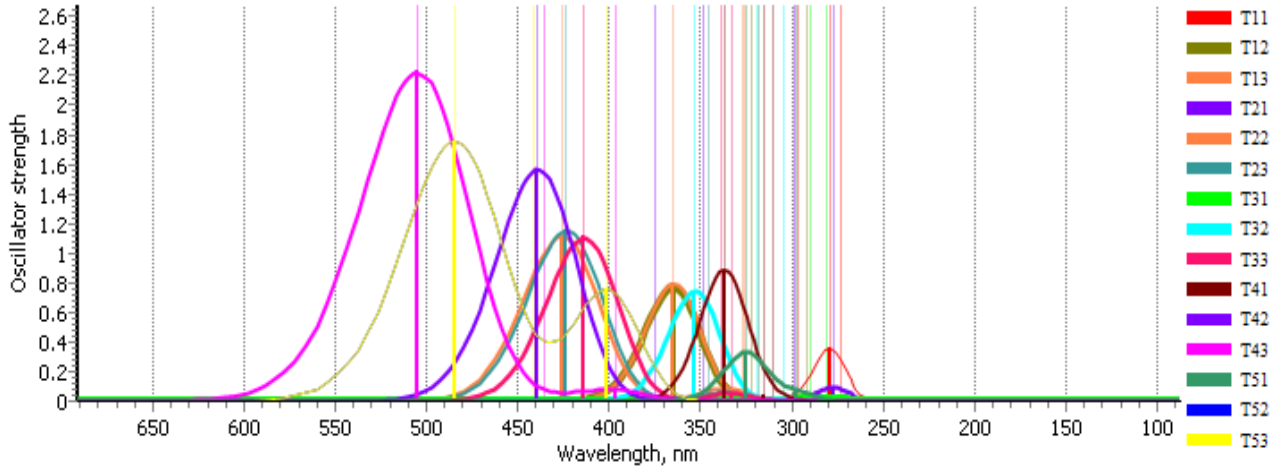


**Figure 9:**Simulated UV-visible optical absorption spectra of each compound of the pyrimidine-(thiophen)n based derivatives at the TD/DFT B3LYP/6-31G(d,p) level.

The calculated absorption wavelengths (λmax) arising from S0→S1 electronic transition increase progressively with the increasing of conjugation lengths in the following orders: O11>O12>O13>, O21>O22>O23, O31>O32>O33, O41>O42>O43 and O51>O52>O53 for pyrimidine-(oxadiazol)n (T11>T12>T13>, T21>T22>T23, T31>T32>T33, T41>T42>T43 and T51>T52>T53 for pyrimidine-(thiophen)n, respectively). It is reasonable, since HOMO→LUMO transition is predominant in S0→S1 electronic transition; the results are a decrease of the LUMO and an increase of the HOMO energy. We typically see a red shift as the conjugation

length increases. We emphasize that the calculated values of λmax are shifted in the same direction upon substitution whatever the substituent's position on the pyrimidine ring.
The increase of the values of the calculated oscillator strengths O.S is obviously due to the bathochromic shift when moving from n=1 to n=3 (depending on the length of conjugation). Therefore, among the pyrimidine-(oxadiazol)n (pyrimidine-(thiophen)n, respectively) derivatives, the molecule O43 (T43, respectively) has the best optic properties which suggest this compound as good candidate for optoelectronic applications. These results show that the performance of solar cells favors better with increasing the length of π conjugated polymer grafted to the pyrimidine ring. Overall the molecules considered in the present study, the molecule T43 has the best optic properties (λmax = 505.11nm, OS= 2.23) which recommend this compound as the best candidate for opto-electronic applications.

## Conclusions

This study has been devoted to a theoretical analysis of the geometries and electronic properties of various compounds based on pyrimidines π-conjugated materials which display the effect of aromatic groups on the electronic structures and optoelectronic properties of these materials and lead to the possibility to suggest these materials for organic solar cells application. We have shown that for the pyrimidine-(polythiophen) and pyrimidine-(polyoxadiazol) derivatives the energy bandgap decreases when the length of the polymer is increased thanks to the effect of the conjugated systems in the studied compounds. The energy bandgap of T43 is much smaller than that of the other compounds. In addition, T43 have a relatively high value of λmax (absorption) along with the strongest O.S and is expected therefore to have the most outstanding optical properties. The obtained properties (small gap and high λmax) suggest these materials are good candidates for optoelectronic applications. All the studied molecules can be used as sensitizers because the electron injection process from the excited molecule to the conduction band of PCBM and the subsequent regeneration are feasible in the organic sensitized solar cell. The quantum chemical calculation procedure, presented in this work, may be used as a model system for understanding the relationships between molecular structure and electronic properties and to predict the electronic properties in addition to design novel materials for organic solar cells application.

**Acknowledgments-**Y. KARZAZI extends his appreciation to the Laboratory for Chemistry of Novel Materials, University of Mons, Belgium, for access to the computational facility.

## References

1. Yan S. G., Lyon L. A., Lemon B. I., Preiskorn J. S., Hupp J. T., *J. Chem. Educ.* 74 (1997) 657.
2. Peet J., Kim J. Y., Coates N. E., Ma W. L., Moses D., Heeger A. J., Bazan G. C., *Nature Materials.* 6 (2007) 500.
3. Karzazi Y., Arbouch I., *J. Mater. Environ. Sci.* 5 (5) (2014) 1505-1515.
4. El Alamy A., Amine A., Bouzzine S. M., Hamidi M., Bouachrine M., *International Journal of Innovation and Scientific Research* 2 (2015) 283.
5. Arbouch I., Karzazi Y., Hammouti B., *Phys. Chem. News*, 72 (2014) 73-84.
6. Servaites J. D., Ratner M. A., Marks T. J., *Energy Environ. Sci*. 4 (2011) 4410.
7. Zhou Hu., Yang Li, You We.,*Macromolecules* 45 (2012) 632.
8. Karzazi Y., *J. Mater. Env. Sci.* 5 (2014) 1.
9. Forrest S. R., *Nature International Weekly Journal of Science*. 29 April (2004) 918.
10. Apilo P., Hiltunen J., Välimäki M., Heinilehto S., Sliz R., Hast J., *Prog. Photovolt: Res. Appl.* 23 (2015) 928.
11. Välimäki M., Apilo P., Po R., Jansson E., Bernardi A., Ylikunnari M., Vilkman M., Corso G., Puustinen J., TuominenaJ., Hasta J., *Nanoscale*, 7 (2015) 9570.
12. Reinhardt J., Apilo P., Zimmermann B., Rousu S., WürfelU., *Solar Energy Materials & Solar Cells* 134 (2015) 164.
13. You J., Dou L., Yoshimura K., Kato T., Ohya K., Moriarty T., Emery K., Chen C-C., Gao J., Li G., *Nature Communications* 4 (2013) 1446.
14. He Z., Zhong C., Su S., Xu M., Wu H., Cao Y., *Nature Photonics*. 6 (2012) 591.
15. Peters CH., Sachs-Quintana I., KastropJP., Beaupre S., Leclerc M., Mcgehee MD., *Advanced Energy Materials*. 1 (2011) 49.

16. Kopola P., Zimmermann B., Filipovic A., SchleiermacherH.-Fr., Greulich J., Rousu S., Hast J., Myllyla R., Wurfel U., *Solar Energy Materials & Solar Cells*. 107 (2012) 258.
17. Roncali J. *Accounts of Chemical Research* 11 (2009) 1730.
18. G. Yu, J. Gao, J. Hummelen, F. Wudl, A. Heeger, *Science-AAAS-Weekly Paper Edition*. 270 (1995) 1789.
19. Becke A. D., *J. Chem. Phys*. 96 (1992) 9489–9497.
20. Becke A. D., *J. Chem. Phys*. 98 (1993) 1372–1377.
21. Lee C., Yang W., Parr R. G., *Phys. Rev. B* 37 (1988) 785–789.
22. Gaussian 09, Revision C.01, M. J. Frisch, G. W. Trucks, H. B. Schlegel, G. E. Scuseria, M. A. Robb, J. R. Cheeseman, G. Scalmani, V. Barone, B. Mennucci, G. A. Petersson, H. Nakatsuji, M. Caricato, X. Li, H. P. Hratchian, A. F. Izmaylov, J. Bloino, G. Zheng, J. L. Sonnenberg, M. Hada, M. Ehara, K. Toyota, R. Fukuda, J. Hasegawa, M. Ishida, T. Nakajima, Y. Honda, O. Kitao, H. Nakai, T. Vreven, J. A. Montgomery, Jr., J. E. Peralta, F. Ogliaro, M. Bearpark, J. J. Heyd, E. Brothers, K. N. Kudin, V. N. Staroverov, T. Keith, R. Kobayashi, J. Normand, K. Raghavachari, A. Rendell, J. C. Burant, S. S. Iyengar, J. Tomasi, M. Cossi, N. Rega, J. M. Millam, M. Klene, J. E. Knox, J. B. Cross, V. Bakken, C. Adamo, J. Jaramillo, R. Gomperts, R. E. Stratmann, O. Yazyev, A. J. Austin, R. Cammi, C. Pomelli, J. W. Ochterski, R. L. Martin, K. Morokuma, V. G. Zakrzewski, G. A. Voth, P. Salvador, J. J. Dannenberg, S. Dapprich, A. D. Daniels, O. Farkas, J. B. Foresman, J. V. Ortiz, J. Cioslowski, and D. J. Fox, Gaussian, Inc., Wallingford CT, (2010).
23. Dennington R., Keith T., Millam J., GaussView, Version 5.0, Semichem Inc. KS, 2005.
24. El alamy A., Amine A., Bouzzine SM., Hamidi M., Bouachrine M. *Mor. J. Chem*. 4 (2015) 697.
25. Z. El Aslaoui, Y. Karzazi, *Mor. J. Chem.* 4 (3) (2016) 838-848.
26. Derouiche H., Djara V., *Sol. Energy Mater. Sol. Cells*, 91 (2007) 1163.
27. Zhang L., Zhang Q., Ren H., Yan H., Zhang J., Zhang H., Gu J., *Sol. Energy Mater. Sol. Cells*. 92 (2008) 581.
28. Bertho S., Haeldermans I., Swinnen A., Moons W., Martens T., Lutsen L., Vanderzande D., Manca J., Senes A., Bonfiglio A., *Energy Mater. Sol. Cells* .91 (2007) 385–389.
29. Gunes S., Neugebauer H., Sariciftci N. S., *Chemical Reviews*. 107 (2007) 1324.
30. Gadisa A., Svensson M., AnderssonM.R., Inganas O., *Appl. Phys. Lett*. 84 (2004) 1609.
31. Scharber M.C., Mühlbacher D., Koppe M., Denk P., Waldauf C., HeegerA.J., BrabecC.J, *Adv. Mater*. 18 (2006) 789.
32. BrabecC.J, Cravino A., Meissner D., SariciftciN.S., Fromherz T., RispensM.T., Sanchez L., Hummelen J.C., *Adv. Funct. Mater*. 11 (2001) 374.
33. Thompson, B. C.; Kim, Y., Reynolds, J. R. *Macromolecules* 38 (2005) 5359.

(2017) ; http://www.jmaterenvironsci.com